



POLITECNICO
MILANO 1863

SCUOLA DI INGEGNERIA INDUSTRIALE
E DELL'INFORMAZIONE

Ray Distribution Aware Heuristics for Bounding Volume Hierarchies Construction

TESI DI LAUREA MAGISTRALE IN
COMPUTER SCIENCE AND ENGINEERING

Author: **Lapo Falcone**

Student ID: 996089

Advisor: Prof. Marco Gribaudo

Academic Year: 2023-24



Abstract

In the last few years, real-time computer graphics have been transitioning from a pipeline based on rasterization to one using ray tracing. Ray tracing makes it possible to accurately simulate the behavior of light rays, enabling developers of graphics content to reproduce high-fidelity scenes without using a plethora of techniques to mimic light transport.

While ray tracing is widely used for off-line rendering, such as for CGI effects in films or animated movies, the same cannot be stated for on-line applications, such as videogames. The main problem with ray tracing is that simulating light transport is computationally expensive, reason why in recent videogames ray tracing is only used on small portions of the scene or to simulate some effects (such as reflections, shadows, or ambient occlusion).

In order to increase the spread of ray tracing in on-line rendering applications too, research is moving in two macro directions.

The first one is to build GPUs with an architecture more suited for ray tracing, such as the RT cores from Ampere Nvidia GPUs.

The second, but not least important one is to design software optimizations to make ray tracing cheaper.

One of the problems that is ubiquitous in the ray tracing environment is to detect collisions between a ray and the geometry of the scene to render. Given the huge amount of primitives present in modern graphic applications, it is necessary to use a data structure to accelerate the ray collision retrieval process. The state-of-the-art structure is the bounding volume hierarchy (BVH), which hierarchically organizes primitives, making it possible to skip entire sections of the scene that are spatially far away from the ray that is being traced during BVH traversal.

In this work we propose two novel heuristics that work in pairs to build higher-quality BVHs, a data structure to make it possible to use them, and a comparative analysis of their performance in different scenarios.

The first heuristic, called **projected area heuristic** (PAH), aims at better estimating the amount of rays that hit each node of the BVH by exploiting some artifacts in the ray distribution in the scene, caused by another optimization used in a previous step of the ray tracing pipeline (namely Monte-Carlo importance sampling).

The second one (**splitting plane facing**) aims at reducing the overlap among nodes of the BVH, consequently reducing the number of intersection tests needed during the BVH traversal phase.

Keywords: Ray tracing, bounding volume hierarchy, BVH

Abstract in Lingua Italiana

Abstract Italiano

Parole chiave: Ray tracing, bounding volume hierarchy, BVH

Contents

Abstract	ii
Abstract in Lingua Italiana	iii
Contents	iv
Introduction	1
1 Chapter one	6
2 Chapter two	7
Bibliography	8
A Collision and Culling Algorithms	9
A.1 Ray-AABB Intersection	9
A.2 Ray-Plane Intersection	11
A.3 Ray-Triangle Intersection	12
A.4 AABB-AABB Intersection	13
A.5 Frustum-AABB Intersection	13
A.5.1 1D Projections Overlapping Test	15
A.6 Point inside AABB Test	16
A.7 Point inside Frustum Test	16
A.8 Point inside 2D Convex Hull Test	17
A.9 2D Convex Hull Culling	18
A.9.1 Vertices inside convex hull	20
A.9.2 Edges intersections	20

A.9.3 Vertices ordering	21
A.10 2D Hull Area Computation	22
List of Figures	23
List of Tables	24
List of Symbols	25
Ringraziamenti	26



Introduction

Why ray tracing?

In the field of computer graphics, we refer to ray tracing as a family of rendering algorithms that simulate light transport in order to transition from a mathematical representation of a scene to an image on the screen.

Conceptually ray tracing is an extremely straightforward technique, that can be summarized in a few steps:

1. Generate a ray of light from a light source;
2. Find out the first object the ray intersects;
3. Compute how much energy is absorbed by the material of the object;
4. Modify the direction of the ray based on the material of the object (for example it may be reflected or refracted);
5. Repeat from 2. until the ray hits the camera;
6. Color the pixel of the camera hit by the ray based on the energy of the ray.

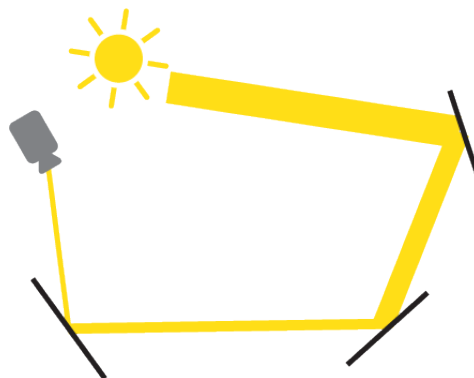


Figure 1: The width of the yellow ray represents the amount of energy carried. After each intersection some energy is absorbed.

Since ray tracing mimics the behavior of light in the real world, the technique can be directly used to simulate complex light effects that would require the use of ad-hoc and

approximate methods if we use other rendering algorithms, such as the widely spread rasterization pipeline.

To give an intuition of how the ad-hoc methods can be convoluted and produce worse results, we summarize one of the most intuitive ones used to generate shadows, called shadow mapping. A shadow map is the projection of the scene from the point of view of a point light source, saved in a texture where each pixel stores the distance from the light source to the projected point. When the scene is projected by the main camera, each visible point is transformed into the coordinate system of the shadow map via matrix multiplication, and is then compared to the point stored in the corresponding pixel of the shadow map. If the point of the shadow map is closer to the light source than the corresponding point projected by the main camera, we deduce that such a point is not visible from the point of view of the light source and, therefore, is in shadow. This specific technique is correct only with point lights, and must be adjusted in case translucent objects are present in the scene.

With ray tracing shadows are natively generated since, if a point is in shadow, no light ray starting from it will hit the camera pixels. Moreover, in principle, it works with any kind of light, not only point lights, and thus produces higher-quality shadows, since no approximations must be made.

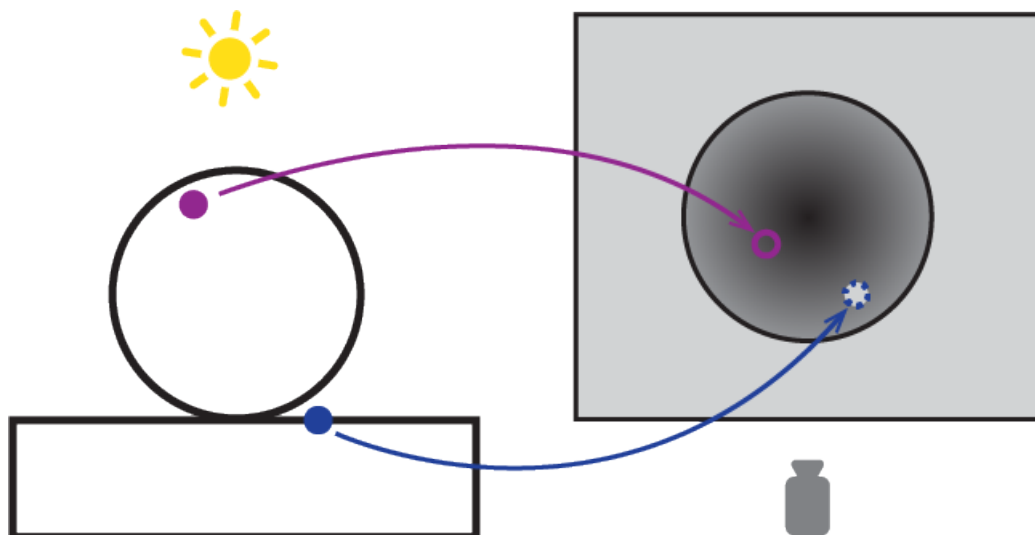


Figure 2: The first figure is from the main camera PoV, the second one from the light source PoV. The second figure represents depth: the closer a point is to the light source, the darker. The blue point is in shadow, because the corresponding point in the shadow map is further away than the stored depth.

We need optimizations

Until now we briefly highlighted the strong points of ray tracing, and greatly simplified

it. The main issue with ray tracing is that it is computationally expensive to simulate light transport. Of course, it is impossible to track the path of every photon emitted by a light source, therefore, even in ray tracing algorithms, some approximations must be made. The nature of the approximations depends on the specific ray tracing algorithm used. For example, in many techniques falling under the name of *backward ray tracing*¹, rays don't start from the light sources, but from the camera, and gain energy when they hit a light source. At this point the path described by the ray is followed backward and the energy hitting the pixel of the camera is computed. In this way the number of rays is greatly reduced, because all the rays hit the camera, therefore none is wasted. On the other hand, some phenomena (such as caustics) cannot be realistically simulated.

From this point on we will consider the scenario where rays are traced backwards.

One optimization that is foundational to modern ray tracing and relevant to our work, is the use of the **Monte-Carlo** integration method, and, in particular, a variance reduction technique called **importance sampling**. We will introduce the concept in this section in an oversimplified way, and then explain it from a mathematical standpoint in ??.

When a ray hits a point on a surface, it may bounce in any direction, based on the material. The most intuitive bounce is a perfect reflection, but, since at a microscopic level surfaces are never perfectly planar, it is possible for the incoming ray to bounce in any direction. This phenomenon is described in a probabilistic way by the bidirectional reflective distribution function (BRDF). Each material is described by a BRDF, and each BRDF makes it more likely for a ray coming from a certain direction to bounce to another range of directions (for example, for a perfectly reflective material, the BRDF will return a probability of 1 for a ray to bounce to the perfect reflection direction).

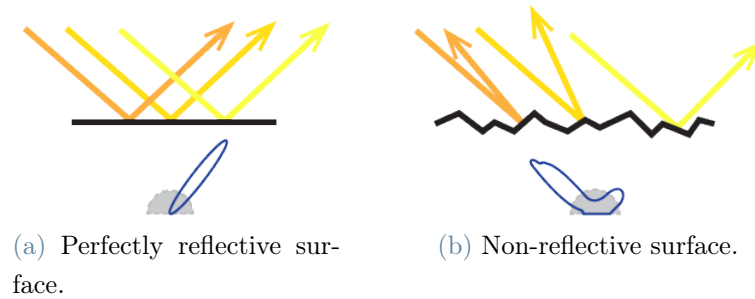


Figure 3: In figure (a) all the rays coming from a direction are reflected towards the same direction. In (b), instead, the surface is microscopically rough, 2 rays coming from the same direction could bounce to 2 very different directions. Under each figure there is the corresponding graph of its BRDF.

¹In some literature the term *backward ray tracing* can also refer to the opposite family of algorithms, since the first ray tracing methods were indeed backward.



Therefore, if we wanted to accurately simulate the light behavior after a ray hits a material, and compute how much light is reflected towards a specific direction (the one of the incoming ray), we would need to send a probe ray to every direction of the hemisphere centered on the hit point, get back the light energy carried by each probe ray, and compute an average based on the probability of each probe ray given by the BRDF. In short, we would need to integrate the light energy function over the hemisphere. This exact same process would then need to be replicated when each probe ray hits an object, recursively, until each ray in the scene hits a light source or gets completely absorbed.

This process, of course, is not feasible, but it can be approximated by the Monte-Carlo method with fewer samples. The idea is that, instead of probing each direction of the hemisphere with a ray, we probe just a small number (often just one) of directions. In most cases the estimate of the light incoming to the point will not be accurate, but, granted that there is a high enough number of incoming rays hitting the neighborhood of the point, the incoming light average will indeed be accurate.

In order to get the most out of the probe rays we cast out of a hemisphere, we would like to send them in directions that contribute the most to final value we are trying to calculate, namely the light reflected toward the direction of the incoming ray. This is the base concept behind importance sampling. In ray tracing there are two common ways to achieve this:

BRDF sampling Probe rays are cast in directions where the BRDF returns a high weight. In this way the energy the probe rays carry is multiplied by a value close to 1; on the other hand, the energy can be a low value.

Light sampling Probe rays are cast directly towards light sources. In this way they will likely carry a lot of energy (unless an obstacle is hit), but the BRDF weight they will be multiplied with may be small.

It is even possible to combine the two techniques with a method called multiple importance sampling (MIS).

The use of importance sampling generates artifacts in the ray distribution on the scene. Rays' directions will no longer be distributed uniformly, but, due to light sampling, more rays will tend to go towards light sources.

Rays intersections

One of the problems that is common to all the algorithms of the ray tracing family is to find the intersection between a ray and the geometry of the scene.

The objects in the scene are usually meshes, which are a collection of geometric primitives.



In many real-world scenarios, primitives are simple triangles, described by 3 vertices. Therefore, the problem of intersecting a ray with the scene is reduced to the problem of intersecting a ray with a collection of triangles.

Given an algorithm to find out if a ray hits a triangle in A.3, the naive way of retrieving the closer triangle hit by a ray would be to perform the ray-triangle test on all the triangles present in the scene. Such an algorithm has a complexity of $\mathcal{O}(n \cdot m)$ where n is the number of triangles and m the number of rays.

Acceleration structures have been developed to speed up the process. The state-of-the-art acceleration structure used in ray tracing is the **bounding volume hierarchy** (BVH).



1 | Chapter one

Chapter 1



2 | Chapter two

Chapter 2



Bibliography

- [1] T. Akenine-Möller, E. Haines, N. Hoffman, A. Pesce, M. Iwanicki, and S. Hillaire. *Real-Time Rendering 4th Edition*. A K Peters/CRC Press, Boca Raton, FL, USA, 2018. ISBN 978-1-13862-700-0. Chapter 22.2.
- [2] G. Gribb and K. Hartmann. Fast extraction of viewing frustum planes from the world-view-projection matrix. *Online document*, 2001.
- [3] Y. Lee and W. Lim. Shoelace formula: Connecting the area of a polygon and the vector cross product. *The Mathematics Teacher*, 110(8):631–636, 2017.
- [4] S. Owen. Ray-plane intersection. https://education.siggraph.org/static/HyperGraph/raytrace/rayplane_intersection.htm, 1999. Accessed: (11/01/2024).
- [5] S. Owen. Ray-box intersection. <https://education.siggraph.org/static/HyperGraph/raytrace/rtinter3.htm>, 2001. Accessed: (10/01/2024).
- [6] S. Oz. Intersection of convex polygons algorithm. <https://www.swtestacademy.com/intersection-convex-polygons-algorithm/>. Accessed: (20/03/2024).
- [7] J.-C. Prunier. Ray-triangle intersection: Geometric solution. <https://www.scratchapixel.com/lessons/3d-basic-rendering/ray-tracing-rendering-a-triangle/ray-triangle-intersection-geometric-solution.html>. Accessed: (09/01/2024).



A | Collision and Culling Algorithms

A.1. Ray-AABB Intersection

The algorithm we used to detect intersections between a ray and an AABB is the branch-less slab algorithm [5].

Given a ray in the form: $r(t) = O + t \cdot d$, where O is the origin and d the direction, the main idea of the algorithm is to find the 2 values of t ($\overline{t_1}$ and $\overline{t_2}$) such that $r(\overline{t_{1,2}})$ are the points where the ray intersects the AABB.

Since the object to intersect the ray with is an axis-aligned bounding box in the min-max form, the algorithm can proceed one dimension at a time:

1. First, it finds the intersection points of the ray with the planes parallel to the yz plane, and sorts them in an ascending order with reference to the corresponding $\overline{t_{1,2}}$ values. We call the point with the smallest \overline{t} value the *closest*, and the other one the *furthest*.
2. Then it does the same with the xz plane:
 - As closest intersection point, it keeps the furthest between the 2 closest intersection points found so far (the one with the yz plane and the one with the xz plane).
 - As furthest intersection point, it keeps the closest between the 2 furthest intersection points found so far.
3. Then it does the same with the xy plane.
4. Finally, an intersection is detected only in the case where the furthest intersection point actually has an associated \overline{t} value bigger than the one of the closest point found by the algorithm.

5. The returned \bar{t} value is the smaller one, as long as it is greater or equal to 0; otherwise it means that the origin of the ray is inside the AABB, and one of the intersection points is *behind* the ray origin.

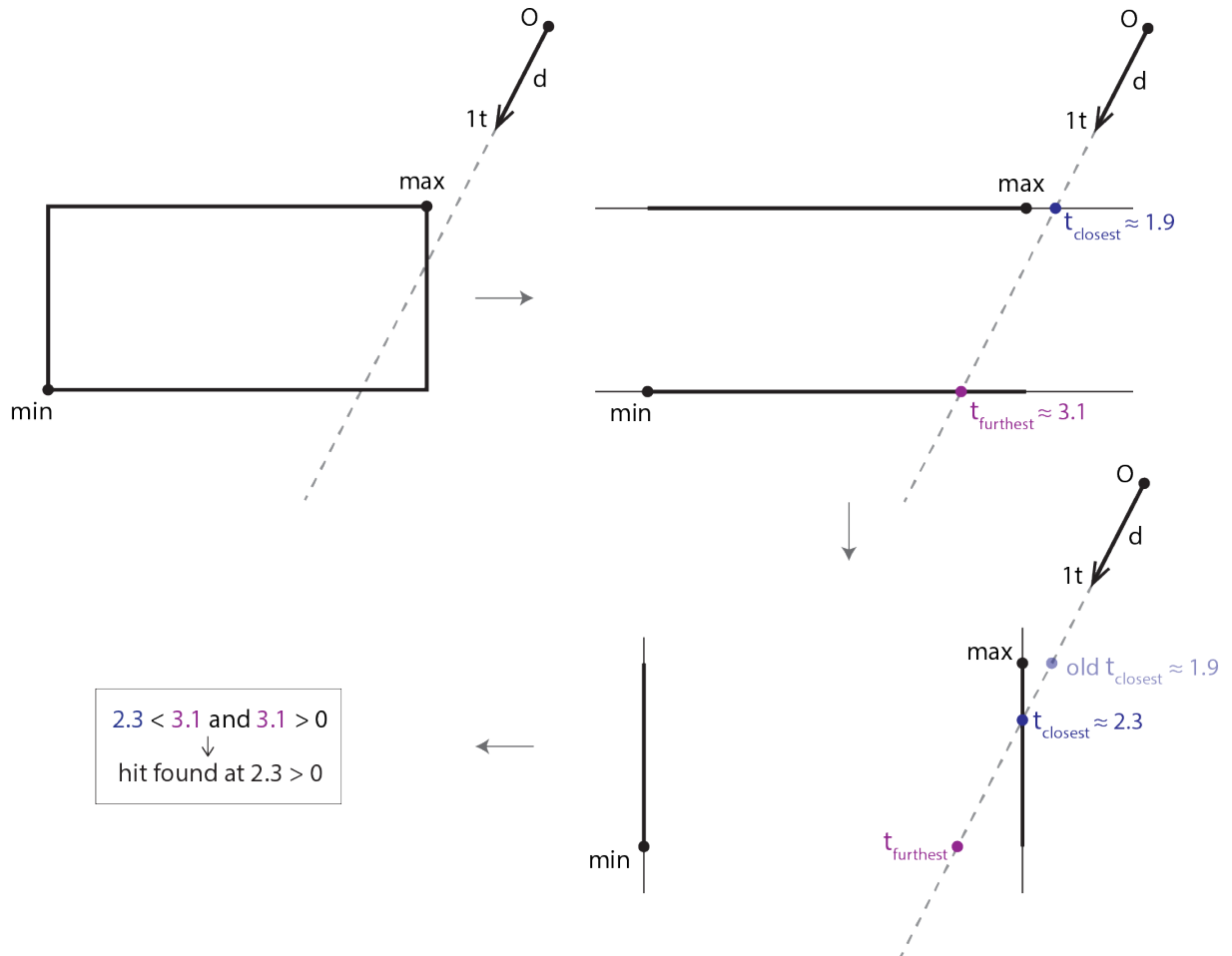


Figure A.1: Visual representation of the presented algorithm in 2 dimensions. An interactive simulation of this algorithm can be found at: <https://www.geogebra.org/m/np3tnjvb>.

Algorithm A.1 Ray-AABB branchless slab intersection algorithm in 3 dimensions

```

1: function INTERSECT(ray, aabb)
2:    $t1_x \leftarrow \frac{aabb.min.x - ray.origin.x}{ray.direction.x}$   $\triangleright$  yz plane
3:    $t2_x \leftarrow \frac{aabb.max.x - ray.origin.x}{ray.direction.x}$ 
4:    $tMin \leftarrow \min(t1_x, t2_x)$ 
5:    $tMax \leftarrow \max(t1_x, t2_x)$ 
6:    $t1_y \leftarrow \frac{aabb.min.y - ray.origin.y}{ray.direction.y}$   $\triangleright$  xz plane
7:    $t2_y \leftarrow \frac{aabb.max.y - ray.origin.y}{ray.direction.y}$ 
8:    $tMin \leftarrow \max(tMin, \min(t1_y, t2_y))$ 
9:    $tMax \leftarrow \min(tMax, \max(t1_y, t2_y))$ 
10:   $t1_z \leftarrow \frac{aabb.min.z - ray.origin.z}{ray.direction.z}$   $\triangleright$  xy plane
11:   $t2_z \leftarrow \frac{aabb.max.z - ray.origin.z}{ray.direction.z}$ 
12:   $tMin \leftarrow \max(tMin, \min(t1_z, t2_z))$ 
13:   $tMax \leftarrow \min(tMax, \max(t1_z, t2_z))$ 
14:   $areColliding \leftarrow tMax > tMin$  and  $tMax \geq 0$ 
15:   $collisionDist \leftarrow tMin < 0 ? tMax : tMin$ 
16:  return  $\langle areColliding, collisionDist \rangle$ 

```

It is interesting to note how, under the floating-point IEEE 754 standard, the algorithm also works when it is not possible to find an intersection point along a certain axis (i.e. when the ray is parallel to certain planes). Indeed, in such cases, the values $\overline{t_{1,2}}$ will be $\pm\infty$, and the comparisons will still be well defined.

A.2. Ray-Plane Intersection

For ray-plane intersection we decided to use this algorithm presented in the educational portal of the SIGGRAPH conference [4].

Given a ray in the form: $r(t) = O + t \cdot d$, where O is the origin and d the direction, and a plane whose normal n and a point P are known, we first check whether the plane and the ray are parallel, in which case no intersection can be found.

Then, if they are not parallel, we obtain the analytic form of the 3-dimensional plane:

$$A \cdot x + B \cdot y + C \cdot z + D = 0$$

In particular, we know a point P that is part of the plane, therefore we can obtain the D

parameter:

$$\begin{aligned} A \cdot P_x + B \cdot P_y + C \cdot P_z + D &= 0 \\ \implies D &= -(A \cdot P_x + B \cdot P_y + C \cdot P_z) \end{aligned}$$

By definition, the vector formed by the parameters $[A, B, C]$ is perpendicular to the plane, therefore:

$$\begin{aligned} D &= -(n_x \cdot P_x + n_y \cdot P_y + n_z \cdot P_z) \\ \implies D &= -\langle n \cdot P \rangle \end{aligned}$$

Now that we have the parametric equation of the plane, we can force a point of the plane to also be a point of the ray:

$$\begin{aligned} A \cdot r(t)_x + B \cdot r(t)_y + C \cdot r(t)_z + D &= 0 \\ \implies A \cdot (O_x + t \cdot d_x) + B \cdot (O_y + t \cdot d_y) + C \cdot (O_z + t \cdot d_z) + D &= 0 \\ \implies t &= \frac{-\langle n \cdot O \rangle + D}{\langle n \cdot d \rangle} \end{aligned}$$

Finally, if the found \bar{t} value is negative, it means that the intersection point between the ray and the plane is *behind* the ray origin, therefore no intersection is found. Else the ray intersects the plane at point $r(\bar{t})$.

Algorithm A.2 Ray-plane intersection algorithm

```

1: function INTERSECT(ray, plane)
2:    $d \leftarrow ray.direction$ 
3:    $O \leftarrow ray.origin$ 
4:    $n \leftarrow plane.normal$ 
5:    $P \leftarrow plane.point$ 
6:   if  $\langle n \cdot d \rangle = 0$  then                                      $\triangleright$  Ray is parallel to plane
7:     return  $\langle false, \_ \rangle$ 
8:    $D \leftarrow -\langle n \cdot P \rangle$ 
9:    $t \leftarrow \frac{-\langle n \cdot O \rangle}{\langle n \cdot d \rangle}$ 
10:  if  $t < 0$  then                                            $\triangleright$  Intersection point is behind ray origin
11:    return  $\langle false, \_ \rangle$ 
12:  else
13:    return  $\langle true, t \rangle$ 

```

A.3. Ray-Triangle Intersection

Once we have algorithms to check for ray-plane intersection (A.2) and for a point inside a 2D convex hull (A.8), we can combine them to check if a ray intersects a triangle and



to compute the coordinates of the intersection point:

1. Build a plane that has as normal the normal to the triangle, and as point any vertex of the triangle;
2. Use the ray-plane intersection algorithm (A.2) to find the coordinates of the point where the ray and the plane collide (if any);
3. Use the point inside 2D convex hull test (A.8) to determine if the intersection point is inside the triangle.

A.4. AABB-AABB Intersection

To detect a collision between 2 axis-aligned bounding boxes in the min-max form, it is sufficient to check that there is an overlap between them in all 3 dimensions. By naming the 2 AABBs as A and B we get:

$$\left\{ \begin{array}{l} A.min_x \leq B.max_x \\ A.max_x \geq B.min_x \\ A.min_y \leq B.max_y \\ A.max_y \geq B.min_y \\ A.min_z \leq B.max_z \\ A.max_z \geq B.min_z \end{array} \right.$$

A.5. Frustum-AABB Intersection

In order to detect an intersection between a frustum and an axis-aligned bounding box in the min-max form, we used a simplified version of the separating axis test (a special case of the separating hyperplane theorem) [1]. The simplification comes from the fact that we need to find the intersection of a frustum and an AABB, and not two 3D convex hulls, meaning that we can exploit some assumptions on the direction of the edges of the two objects, as we'll note below.

Before proceeding with the separating axis test, we first try a simpler AABB-AABB collision test, between the given AABB and the AABB that most tightly encloses the frustum. In case this *rejection test* gives a negative answer, we can deduce that the frustum and the AABB are not colliding. Otherwise, we must use the more expensive SAT.

The separating axis theorem in 3 dimensions states that 2 convex hulls are not colliding if and only if there is a plane that divides the space into 2 half-spaces each fully containing one of the two convex hulls.

To find whether such a plane exists, we project the two convex hulls on certain axes, and check whether their 1D projections are overlapping. The theorem also states that if there is an axis where the projections are not overlapping it must be either:

- An axis perpendicular to one of the faces of the convex hulls, or
- An axis parallel to the cross product between an edge of the first convex hull and an edge of the second convex hull.

This consideration makes it possible to use the theorem in a concrete scenario.

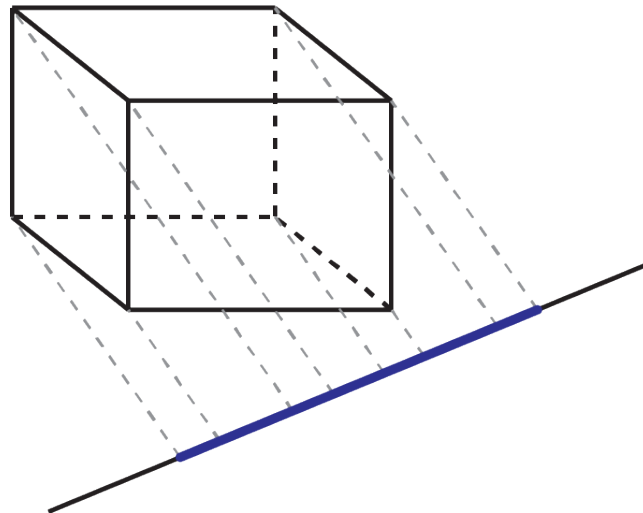


Figure A.2: The projection of an AABB on an axis.

In principle, given 2 polyhedra with 6 faces each (such as a frustum and an AABB), there should be $(6 + 6)_{normals} + (12 \cdot 12)_{cross\ products} = 156$ axis to check; but, since:

- The AABB has edges only in 3 different directions, and faces normals only in 3 different directions, and
- The frustum has edges only in 6 different directions, and faces normals only in 5 different directions

the number of checks is reduced to $(3 + 5)_{normals} + (3 \cdot 6)_{cross\ products} = 26$.

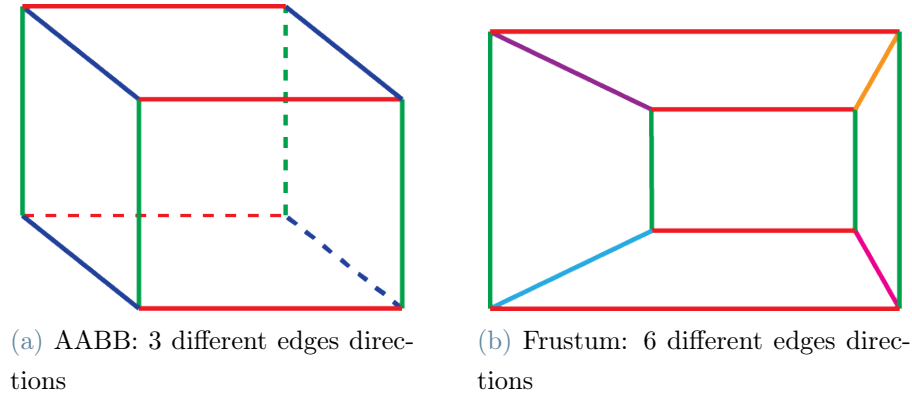
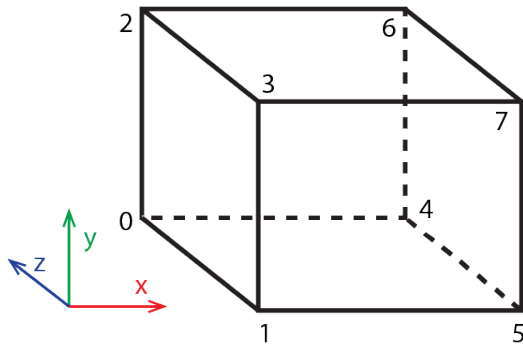


Figure A.3: In the figure the edges having the same direction are colored in the same color.

A.5.1. 1D Projections Overlapping Test

In order to detect if the 1D projections of the 3D hulls are overlapping, we identify the outermost points of each projection (namely A_{min} , A_{max} , B_{min} , B_{max}) and check that $B_{min} \leq A_{max}$ & $B_{max} \geq A_{min}$.

For the AABB another optimization is possible, where we detect what points will be the outermost after the projection without actually projecting them, based on the direction of the axis:



(a) AABB vertices layout.

axis direction	extremes
$x \geq 0 \ \& \ y \geq 0 \ \& \ z \leq 0$	1, 6
$x \leq 0 \ \& \ y \leq 0 \ \& \ z \geq 0$	6, 1
$x \geq 0 \ \& \ y \geq 0 \ \& \ z \geq 0$	0, 7
$x \leq 0 \ \& \ y \leq 0 \ \& \ z \leq 0$	7, 0
$x \geq 0 \ \& \ y \leq 0 \ \& \ z \leq 0$	3, 4
$x \leq 0 \ \& \ y \geq 0 \ \& \ z \geq 0$	4, 3
$x \geq 0 \ \& \ y \leq 0 \ \& \ z \geq 0$	2, 5
$x \leq 0 \ \& \ y \geq 0 \ \& \ z \leq 0$	5, 2

Algorithm A.3 Ray-AABB branchless slab intersection algorithm in 3 dimensions

```

1: function INTERSECT(frustum, aabb)
2:   if !intersect(frustum.aabb, aabb) then ▷ AABB-AABB test
3:     return false
4:   axesToCheck ← (⊥ frustum faces) ∪ (⊥ AABB faces) ∪ (×edges)
5:   for all axis ∈ axesToCheck do
6:     frustumExtremes ← findFrustumExtremes(frustum, axis) ▷ Returns the
       vertices of the frustum that, after the projection, will be the extremes
7:     aabbExtremes ← findAabbExtremes(aabb, axis) ▷ Same as above, but uses
       the discussed optimization
8:      $A_{min} \leftarrow \langle aabbExtremes.first \cdot axis \rangle$ 
9:      $A_{max} \leftarrow \langle aabbExtremes.second \cdot axis \rangle$ 
10:     $B_{min} \leftarrow \langle frustumExtremes.first \cdot axis \rangle$ 
11:     $B_{max} \leftarrow \langle frustumExtremes.second \cdot axis \rangle$ 
12:    if !( $B_{min} \leq A_{max}$  &  $B_{max} \geq A_{min}$ ) then
13:      return false
14:  return true ▷ If we haven't found any axis where there is no overlap, boxes are
       colliding

```

A.6. Point inside AABB Test

To check if a point P is inside an axis-aligned bounding box in the min-max form, it is sufficient to compare its coordinates with the minimum and maximum of the AABB component-wise:

$$\begin{cases} min_x \leq P_x \leq max_x \\ min_y \leq P_y \leq max_y \\ min_z \leq P_z \leq max_z \end{cases}$$

A.7. Point inside Frustum Test

It is possible to detect whether a point is inside a 3-dimensional frustum by projecting it with the perspective matrix associated with the frustum and then comparing its coordinates, as suggested by [2].

Given the perspective matrix M associated with the frustum, we can project a point P and get: $P' = M \cdot P$; and perform the perspective division.

$P'' = \frac{P'}{P'_w}$ P'' is now in normalized device coordinates (NDC) space, where the frustum is

an axis-aligned bounding box that extends from $\langle -1, -1, -1 \rangle$ to $\langle 1, 1, 1 \rangle$ ¹.

It is now immediate to see that P is inside the frustum if and only if P'' is inside the AABB (see section A.6).

A simple optimization allow us to avoid the perspective division. Indeed, since in homogeneous coordinates:

$$\langle x', y', z', w' \rangle = \left\langle \frac{x'}{w'}, \frac{y'}{w'}, \frac{z'}{w'}, \frac{w'}{w'} \right\rangle = \langle x'', y'', z'', 1 \rangle$$

We can change the inequalities to check whether the point is inside the frustum from:

$$\begin{cases} -1 \leq x'' \leq 1 \\ -1 \leq y'' \leq 1 \\ -1 \leq z'' \leq 1 \end{cases} \quad \text{to:} \quad \begin{cases} -w' \leq x' \leq w' \\ -w' \leq y' \leq w' \\ -w' \leq z' \leq w' \end{cases}$$

We created a 2D visual demonstration of how it is possible to detect if a point is inside a frustum at <https://www.geogebra.org/m/ammj5mxd>.

A.8. Point inside 2D Convex Hull Test

Given a 2D convex hull in 3-dimensional space and a 3D point laying on the same plane as the hull, it is possible to use a simple inside-outside test [7] to determine whether the point is inside the convex hull.

The main idea is that the point lays inside the convex hull if and only if it is *to the right* (or *to the left*, depending on the winding order) of all the edges of the hull.

In order to determine the relative position of a point and an edge \overline{AB} , we can look at the cross product:

$$u \times v \text{ where } u = \overrightarrow{AB}, v = \overrightarrow{AP}$$

¹Based on the convention used, it is possible that the AABB in NDC space has a different size. For example, it is common an AABB extending from $\langle -1, -1, 0 \rangle$ to $\langle 1, 1, 1 \rangle$

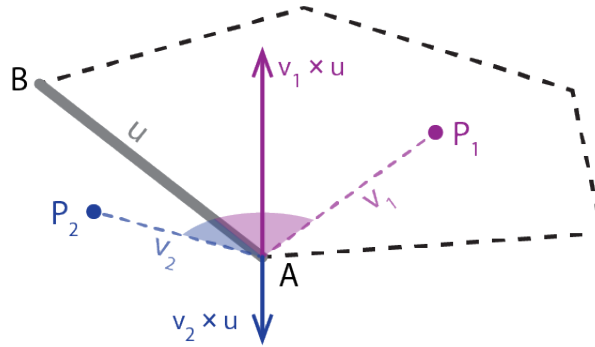


Figure A.4: Visualization of cross product.

Therefore the strategy to determine if a point is on the same side of all the edges of the convex hull is to compute a reference cross product, by choosing any of the edges, and then making sure that all the other cross products have the same direction. To check that 2 vectors have the same direction it is sufficient that their dot product is positive.

Algorithm A.4 Inside-outside test between a 3D point and a 2D convex hull.

```

1: function ISINSIDE( $P, hull$ )
2:    $N \leftarrow$  number of edges of hull
3:    $u \leftarrow hull[0] - hull[N - 1]$ 
4:    $v \leftarrow P - hull[N - 1]$ 
5:    $ref \leftarrow u \times v$   $\triangleright$  The reference cross product
6:   for  $0 \leq i < N$  do
7:      $u \leftarrow hull[i + 1] - hull[i]$ 
8:      $v \leftarrow P - hull[i]$ 
9:      $cross \leftarrow u \times v$ 
10:    if  $\langle ref \cdot cross \rangle \leq 0$  then
11:      return false
12:  return true

```

A.9. 2D Convex Hull Culling

In order to find the overlapping region between two 2D hulls in 2-dimensional space, we can proceed as illustrated in the diagram below ([6]):

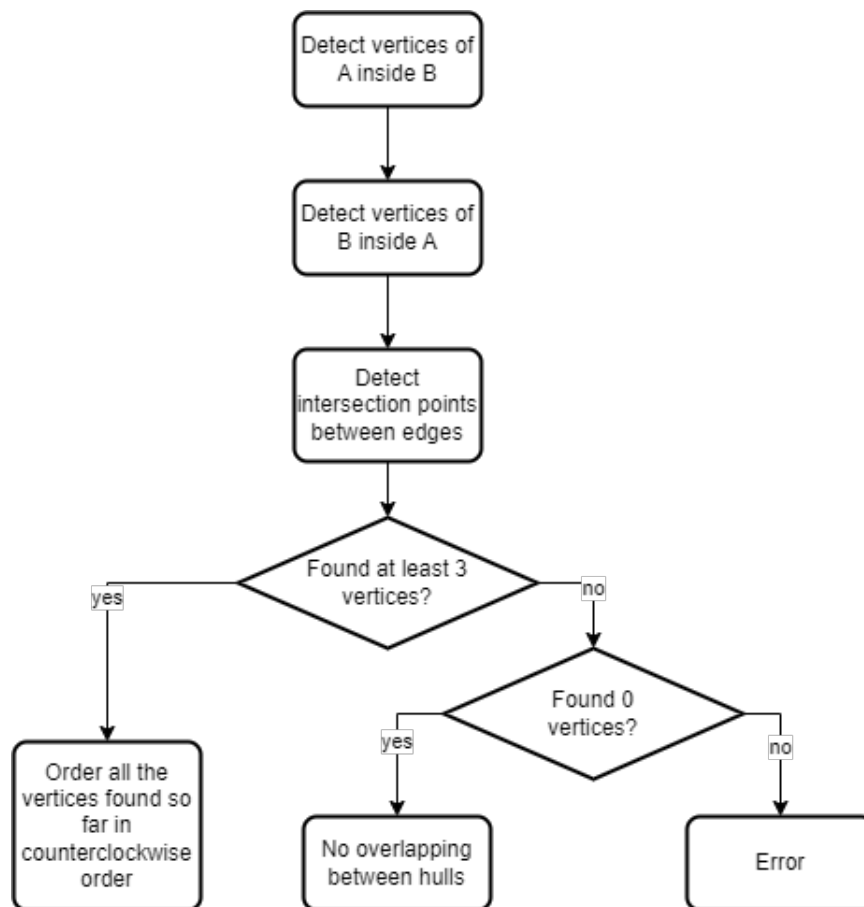


Figure A.5: General algorithm to find the overlapping region between two convex hulls called A and B .

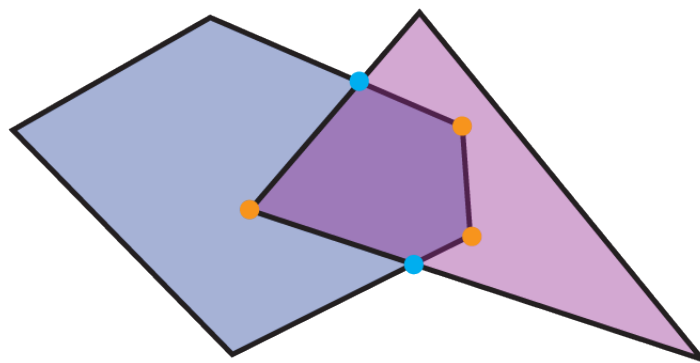


Figure A.6: Yellow vertices are found in the first 2 steps (vertices inside), whereas light blue vertices are found in the third step (edges intersections).

We'll now go through each phase and see the used algorithms.

A.9.1. Vertices inside convex hull

To find out what vertices of a hull are inside the other one we simply looped over them and used the point inside convex hull test (A.8).

A.9.2. Edges intersections

To detect an intersection between two segments, we first have to compute the equation of the line the segment is lying on.

Given a segment \overline{PQ} , the underlying line has equation:

$$A \cdot x + B \cdot y = C$$

We can then compute the parameters of the line as:

$$\begin{cases} A = Q_y - P_y \\ B = P_x - Q_x \\ C = A \cdot P_x + B \cdot P_y \end{cases}$$

After we calculate the underlying line of both segments, with parameters $A_1, B_1, C_1, A_2, B_2, C_2$, we can compute the intersection point K of the two lines as:

$$\begin{cases} \Delta = A_1 \cdot B_2 - A_2 \cdot B_1 \\ K_x = \frac{B_2 \cdot C_1 - B_1 \cdot C_2}{\Delta} \\ K_y = \frac{A_1 \cdot C_2 - A_2 \cdot C_1}{\Delta} \end{cases}$$

We are now left with the task of verifying whether the found intersection point K is in between both segments' extremes. Let's call the first segment \overline{MN} and the second one \overline{PQ} :

$$\begin{cases} \min(M_x, N_x) \leq K_x & \& \\ \max(M_x, N_x) \geq K_x & \& \\ \min(M_y, N_y) \leq K_y & \& \\ \max(M_y, N_y) \geq K_y \end{cases} \quad \text{And} \quad \begin{cases} \min(P_x, Q_x) \leq K_x & \& \\ \max(P_x, Q_x) \geq K_x & \& \\ \min(P_y, Q_y) \leq K_y & \& \\ \max(P_y, Q_y) \geq K_y \end{cases}$$

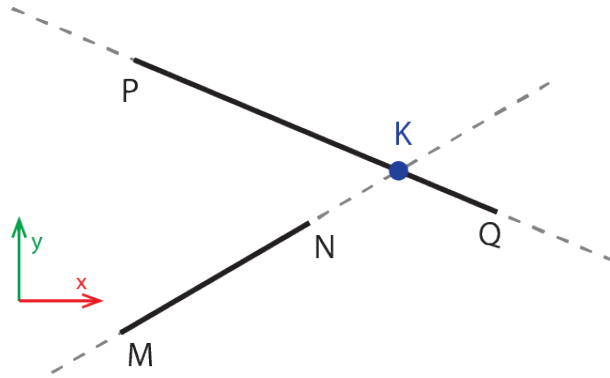


Figure A.7: In this example segments do not collide because $\max(M_x, N_x) = N_x \not\geq K_x$ or $\max(M_y, N_y) \not\geq K_y$

A.9.3. Vertices ordering

Given a set of unordered 2D points belonging to a convex hull, we want to sort them in a counterclockwise order, so that two consecutive vertices form an edge of the convex hull.

To do so we can compute the barycenter O of the set of points that, being them part of a convex hull², is necessarily inside the convex hull itself.

Now, for each vertex A_k we can calculate the vector $\overrightarrow{OA_k}$, and sort the vertices based on $\text{atan2}(\overrightarrow{OA_{k_y}}, \overrightarrow{OA_{k_x}})$.

The $\text{atan2}(v_y, v_x)$ function returns the angle between the positive x-axis and the vector $v = \langle v_x, v_y \rangle$. Differently from the arctangent function, the returned angle ranges in the interval $(-\pi, \pi]$, therefore is well suited for our purpose of sorting the convex hull vertices.

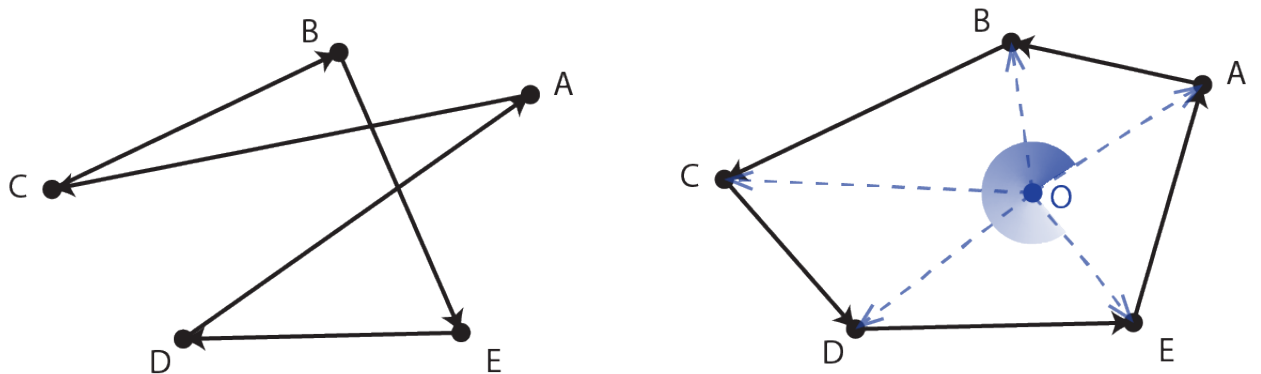


Figure A.8: Vertices of a convex hull before and after atan2 sorting.

²We can state that the vertices we found so far make up a convex hull because the overlapping of two convex hulls is necessarily a convex hull.

A.10. 2D Hull Area Computation

To calculate the area of a 2-dimensional hull we decided to use the Gauss's area formula, also known as the shoelace formula [3].

Given a polygon with vertices P_0, P_1, \dots, P_n , where each vertex has coordinates: $P_k = (x_k, y_k)$, its area can be found with this formula:

$$\begin{aligned}
 Area &= \left| \frac{1}{2} \cdot \left(\begin{vmatrix} x_0 & y_1 \\ y_0 & y_1 \end{vmatrix} + \begin{vmatrix} x_1 & y_2 \\ y_1 & y_2 \end{vmatrix} + \dots + \begin{vmatrix} x_{n-1} & y_n \\ y_{n-1} & y_n \end{vmatrix} + \begin{vmatrix} x_n & y_0 \\ y_n & y_0 \end{vmatrix} \right) \right| \\
 &= \left| \frac{\sum_{i=0}^n (x_i \cdot y_{i+1} - y_i \cdot x_{i+1})}{2} \right|
 \end{aligned}$$

In the last formula we consider $P_0 = P_{n+1}$.

List of Figures

1	The width of the yellow ray represents the amount of energy carried. After each intersection some energy is absorbed.	1
2	The first figure is from the main camera PoV, the second one from the light source PoV. The second figure represents depth: the closer a point is to the light source, the darker. The blue point is in shadow, because the corresponding point in the shadow map is further away than the stored depth.	2
3	In figure (a) all the rays coming from a direction are reflected towards the same direction. In (b), instead, the surface is microscopically rough, 2 rays coming from the same direction could bounce to 2 very different directions. Under each figure there is the corresponding graph of its BRDF.	3
A.1	Visual representation of the presented algorithm in 2 dimensions. An interactive simulation of this algorithm can be found at: https://www.geogebra.org/m/np3tnjvb	10
A.2	The projection of an AABB on an axis.	14
A.3	In the figure the edges having the same direction are colored in the same color.	15
A.4	Visualization of cross product.	18
A.5	General algorithm to find the overlapping region between two convex hulls called A and B	19
A.6	Yellow vertices are found in the first 2 steps (vertices inside), whereas light blue vertices are found in the third step (edges intersections).	19
A.7	In this example segments do not collide because $\max(M_x, N_x) = N_x \not\leq K_x$ or $\max(M_y, N_y) \not\leq K_y$	21
A.8	Vertices of a convex hull before and after <i>atan2</i> sorting.	21



List of Tables



List of Symbols

Symbol	Description	Unit
<i>alpha</i>	symbol 1	km

Ringraziamenti

Lorem ipsum dolor sit amet, consectetur adipiscing elit, sed do eiusmod tempor incididunt ut labore et dolore magna aliqua. Ultricies integer quis auctor elit sed vulputate mi. Accumsan sit amet nulla facilisi morbi. Suspendisse potenti nullam ac tortor vitae purus faucibus. Ultricies lacus sed turpis tincidunt id. Sit amet mauris commodo quis imperdiet. Arcu bibendum at varius vel. Venenatis urna cursus eget nunc. Mus mauris vitae ultricies leo integer malesuada nunc vel. Sodales neque sodales ut etiam sit. Pellentesque dignissim enim sit amet venenatis urna cursus eget nunc. Condimentum mattis pellentesque id nibh tortor id aliquet lectus. Ultrices gravida dictum fusce ut placerat orci nulla pellentesque dignissim. Faucibus pulvinar elementum integer enim neque. Morbi tincidunt augue interdum velit euismod in pellentesque massa.

A diam maecenas sed enim ut sem viverra aliquet eget. Viverra aliquet eget sit amet tellus cras. Tellus at urna condimentum mattis pellentesque. Quis viverra nibh cras pulvinar. Posuere morbi leo urna molestie at elementum. Aenean euismod elementum nisi quis eleifend quam. In hac habitasse platea dictumst vestibulum rhoncus. Nullam non nisi est sit amet facilisis magna etiam tempor. Neque laoreet suspendisse interdum consectetur libero. Vitae auctor eu augue ut lectus arcu bibendum. Ipsum consequat nisl vel pretium lectus quam. Velit dignissim sodales ut eu sem. Odio morbi quis commodo odio. Lectus nulla at volutpat diam. Neque gravida in fermentum et sollicitudin ac. Nunc non blandit massa enim nec dui nunc. Quisque id diam vel quam elementum pulvinar etiam non quam. Consequat id porta nibh venenatis cras sed felis. Vitae justo eget magna fermentum iaculis eu non diam. Mi sit amet mauris commodo.

